THE ASTROPHYSICAL JOURNAL, 392:284–288, 1992 June 10

VACUUM ULTRAVIOLET EXTINCTION MEASUREMENTS ON COSMIC DUST ANALOG CARBON GRAINS

L. COLANGELI
Dipartimento Ingegneria Industriale, Università degli Studi di Cassino, Via Zamosch, n. 43, 03043 Cassino, Italy
A. BLANCO AND S. FONTI
Physics Department, Università di Lecce, Via per Arnesano, 73100 Lecce, Italy
AND
E. BUSSOLETTI
Istituto Universitario Navale, Via A. De Gasperi, n. 5, 80133 Naples, Italy and
Osservatorio Astronomico di Capodimonte, Naples, Italy
Received 1990 October 25; accepted 1991 November 6

ABSTRACT

In this paper we present the results of new systematic spectroscopic analyses performed in the vacuum ultraviolet spectral range (110–300 nm) on amorphous carbon grains produced under different and controlled physical conditions and with two different production methods. The results confirm that particles similar to those obtained in the laboratory might reproduce the extinction observed toward a class of stellar sources characterized by an absorption "bump" at around 240 nm. The 220 nm interstellar hump is not reproduced by laboratory particles. However, a form of the same carbonaceous grains, partially modified in the chemical, structural, and/or morphological properties, may be used to simulate the interstellar extinction curve.

Subject headings: dust, extinction — techniques: spectroscopic — ultraviolet: interstellar

1. INTRODUCTION

The study of interstellar and circumstellar extinction allows one to determine the sizes and the chemical composition of cosmic dust, both in formation environments and in the interstellar medium, and to better understand the mechanisms involved in the dust/gas relations. However, in spite of the large amount of available observational data, the true composition of cosmic dust is far from being completely settled.

Interstellar extinction curves measured toward a large number of sources typically exhibit a 220 nm extinction "bump" followed by a minimum of extinction and a steep rise in the far-UV. Furthermore, the absence of fine structures limits the range of candidates for the absorbing materials.

In the diffuse interstellar medium, the overall shape of the extinction curves appears to be rather uniform over relatively large areas (100 × 100 pc). Nevertheless, the so-called mean interstellar extinction curve has now become obsolete since recent observations (Massa & Savage 1989) have shown a relevant variability in the profile of UV extinction curves from one line of sight to another. Therefore, it appears more reasonable to study the behavior of extinction in well-localized regions.

On the other hand, the extinction produced by dust in its formation regions seems to be rather different from that observed in the interstellar curves. In fact, some sources, for example, Abell 30 (Greenstein 1981), RCrB and RY Sgr (Hecht et al. 1984), and HD 213985 (Buss, Lamers, & Snow 1989), have an absorption "bump" at 230–250 nm, while other objects such as α Sco (Snow et al. 1987) and HD 89353 (Buss et al. 1989) do not show any detectable absorption band.

Many authors have interpreted both the interstellar and the circumstellar 220–250 nm features with the presence of carbon-based grains (Stecher & Donn 1965; Gilra 1972; Mathis, Rumpl, & Nordsieck 1977; Hong & Greenberg 1980; Draine & Lee 1984; Hecht 1986; Buss et al. 1989; Wright 1989). In particular, amorphous carbon grains may play an important role (Czyzak & Santiago 1973; Yamamoto & Hasegawa 1977; Seki & Hasegawa 1981; Czyzak, Hirth, & Tabak 1982). Other explanations based on noncarbonaceous materials remain more uncertain (Duley, Jones, & Williams 1989; Draine 1989).

On the other hand, the far-UV extinction rise could be due either to scattering from very small grains (see, e.g., Greenberg 1986) or to absorption from hydrogenated amorphous carbon particles (Hecht 1986). Furthermore, according to the computations performed by Lewis, Anders, & Draine (1989), the presence of diamond-like carbonaceous particles could contribute to the profile of the extinction rise.

More information is needed in order to determine the structural (amorphous and/or crystalline), chemical (hydrogenated or dehydrogenated), and morphological (single or clustered grains) status of the dust. In this respect, laboratory investigation on cosmic dust analogues can be of great help in interpreting astronomical observations and in supporting the theoretical simulations.

Morphological and spectroscopic analyses on various kinds of amorphous carbon solid particles, produced in the laboratory, have been performed in the past (Stephens 1980; Koike, Hasegawa, & Manabe 1980; Bussoletti et al. 1987a, and references therein). In particular, Colangeli et al. (1986) have already measured the UV extinction of a limited number of amorphous carbon samples. In this paper, we present the results of new systematic analyses performed on a larger set of samples. The grains have been produced under different and controlled physical conditions in order to clarify the influence of some parameters (production method, ambient pressure, collecting distance, amount of mass deposit) on the final optical properties. Although the data seem to confirm previous general findings, some new results are presented.

2. EXPERIMENTAL

Vacuum ultraviolet extinction measurements were performed at room temperature in the wavelength range from 110 to 300 nm by using the PULS synchrotron light facility of the INFN National Laboratory in Frascati (Rome). The lower wavelength limit was imposed by the transmission cutoff of the lithium fluoride (LiF) substrates used in our measurements. A Hilger Watts vacuum monochromator ($\simeq 10^{-9}$ Torr) allowed us to analyze the synchrotron light coming from the storage ring ($E = 1.5$ GeV; $I \simeq 50$ mA) and to focus the beam (1 mm^2 spot) onto the samples. A grating with 1440 lines mm^{-1} and linear dispersion of 0.5 nm mm^{-1} was used in the range 110–140 nm. A Bendix detector without any filter allowed us to collect the sample signal. We covered the remaining range of interest up to 300 nm by means of a second grating with 600 lines mm^{-1} and linear dispersion 1.2 nm mm^{-1} together with a photomultiplier (RCA C70128) fitted with a LiF input window. A quartz filter was inserted to suppress the higher diffraction orders in the 150–300 nm range.

A mirror positioned between the monochromator and the sample chamber sent a fraction of the light beam onto a second photomultiplier (reference signal). Both the sample and the reference signals were amplified by standard lock-in techniques; the data were collected and preliminarly analyzed by means of an on-line computer.

The amorphous carbon grains studied in our investigation were prepared by (1) arc discharge in Ar gas (AC samples) and (2) benzene burning in air (BE samples). These techniques have been described already in previous papers to which we refer for further details (i.e., Bussoletti et al. 1987a). Spheroidal solid grains with average radii $\langle a \rangle = 40$ Å for AC samples and $\langle a \rangle = 150$ Å for BE samples, respectively, were produced.

The arc discharge occurred between two amorphous carbon electrodes in an inert Ar atmosphere. Several dust samples were collected onto LiF substrates by varying the following parameters: (1) collecting distance from the arc (3, 5, 10 cm); (2) pressure conditions ($p = 10$ and 20 mbar); and (3) amount of collected mass. We have chosen the transmission at around 245 nm, where a well-pronounced extinction peak is detected, as an indicator of the dust amount collected per unit area. The BE samples were produced in air at room conditions. A summary of the samples prepared and analyzed in the vacuum UV is reported in Table 1. It is worthwhile to point out that only half of each LiF substrate was covered by grains in order to measure separately both the transmission of the substrate and that of the substrate plus dust.

TABLE 1

UV Spectral Characteristics of Amorphous Carbon Samples Analyzed in the Vacuum UV Spectral Range

Sample	d (cm)	p (mbar)	$T(\lambda_P)$	λ_P (nm)	λ_M (nm)	α
AC3A7	3	10	80%	248	176	2.4
AC3H9	3	10	60	248	187	2.4
AC3H6	3	10	25	243	173	2.4
AC5A6	5	10	80	245	180	3.0
AC5H5	5	10	60	242	170	2.4
AC5H2	5	20	60	246	172	2.5
AC10H4	10	10	80	248	175	[a]
BE5H7	5	1033	60	260	165	2.1

Notes.—d = collecting distance; p = pressure; $T(\lambda_P)$ = measured transmission at the peak position; λ_P = wavelength position of the bump; λ_M = wavelength position of the UV minimum; α = spectral index at $\lambda \leq 160$ nm.

[a] Secondary peak at $\lambda \simeq 160$ nm.

3. RESULTS

Several independent extinction measurements at the same sample position have been performed for the samples listed in Table 1 in order to investigate the potential influence of various production parameters on the extinction properties of the carbon grains. Furthermore, in some cases the incident beam has been focused on different points of the sample in order to check the homogeneity both of the substrate and of the dust deposit. We found a good agreement between the results of different scans, within the experimental errors, so that we report here average extinction curves.

In Figures 1 to 3 the value $\ln(1/T)$ is plotted versus wavelength for all the analyzed samples. Here T represents the ratio T_1/T_2, where T_1 and T_2 are, respectively, the transmittance of the portion of LiF substrate covered with dust and the transmittance of the half "blank" substrate. This approach was used because some differences in the transmittance profile of blank substrates have been detected; they might introduce errors in the determination of the actual transmittance of the dust unless T_1 data are normalized to their own T_2 substrate data. Therefore, the plotted function is proportional to the extinction efficiency of the dust.

By looking at the spectra reported in Figures 1–3 we can identify some features common to all the amorphous carbon samples:

1. A wide "bump" falling at $\lambda_P \simeq 240$–250 nm for AC and at $\lambda_P \simeq 260$ nm for BE samples;

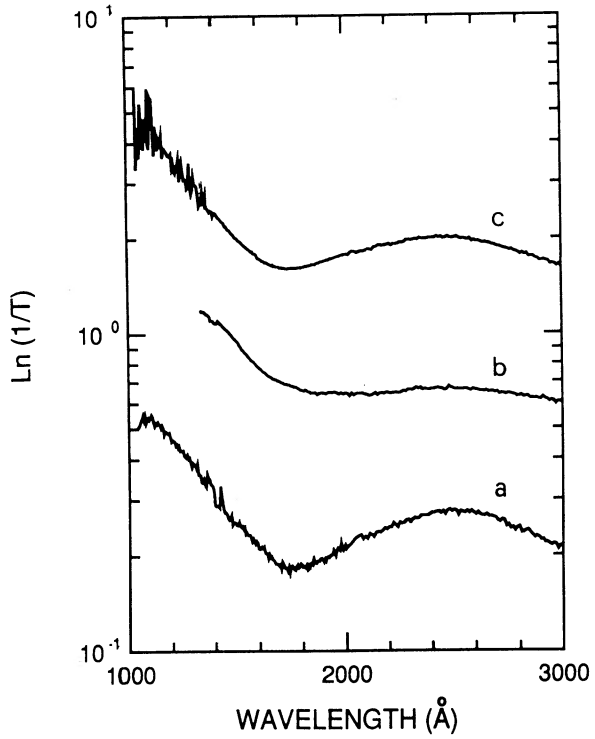

Fig. 1.—The $\ln(1/T)$ vs. wavelength computed from laboratory transmission data for amorphous carbon samples collected at 3 cm from the arc which contain different dust mass amounts: (*a*) AC3A7, (*b*) AC3H9, and (*c*) AC3H6 (*see also Table 1*). All these samples were produced at a pressure of 10 mbar.

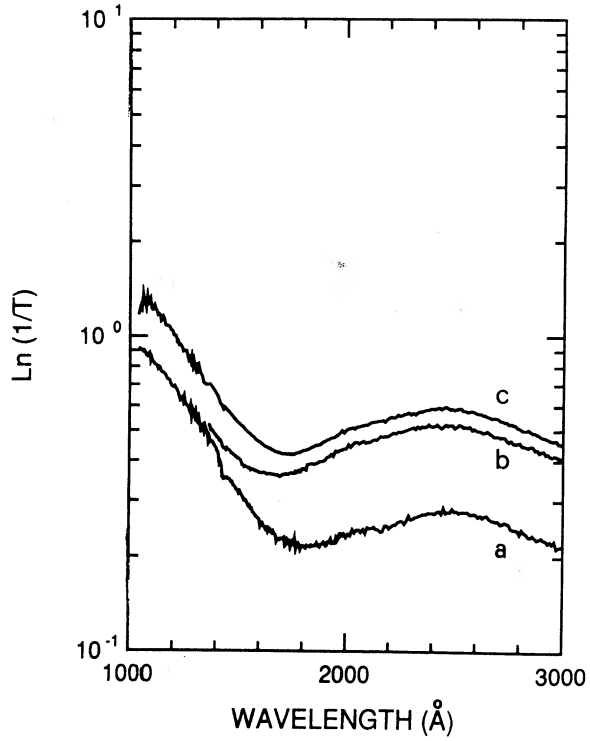

FIG. 2.—The $\ln(1/T)$ vs. wavelength computed from laboratory transmission data for amorphous carbon samples collected at 5 cm from the arc which contain different dust mass amounts: (*a*) AC5A6, (*b*) AC5H5, and (*c*) AC5H2 (*see also Table 1*). Samples AC5A6 and AC5H5 were produced at a pressure $p = 10$ mbar, while sample AC5H2 was produced at $p = 20$ mbar.

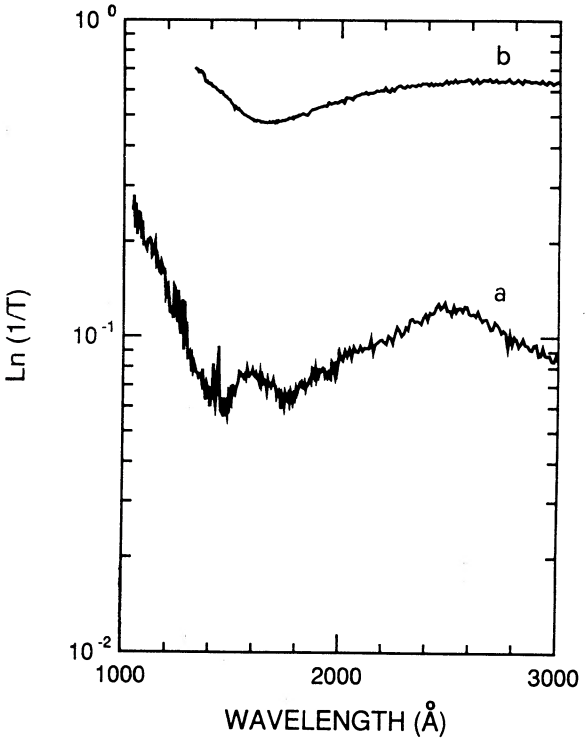

FIG. 3.—The $\ln(1/T)$ vs. wavelength computed from laboratory transmission data for (*a*) the amorphous carbon sample collected at 10 cm from the arc at a pressure $p = 10$ mbar (AC10H4); and (*b*) for the sample produced by benzene burning at normal conditions (BE5H7).

2. A minimum of extinction which, for most samples, lies between $\lambda_M = 170$ and 180 nm;

3. A steep rise for $\lambda \leq 160$ nm that can be fitted by a $\lambda^{-\alpha}$ power law with typical spectral index $\alpha \simeq 2.4$.

All the major spectral characteristics of each sample are summarized in Table 1.

Some differences can be identified from sample to sample. First of all we have to observe that, in agreement with previous results (Stephens 1980; Koike et al. 1980; Borghesi, Bussoletti, & Colangeli 1985; Colangeli et al. 1986), all the AC samples show the "hump" falling around 240–250 nm, while the BE sample shows a broader feature shifted to 260 nm. On the other hand, differences in the profile of the peak appear evident even between AC samples. In particular, the humps in the AC3H9 and AC10H4 samples are, respectively, shallower and sharper than in the other spectra.

The position of the minimum in the extinction curves is not stable and varies between the limits 170 and 180 nm. Only in the AC3H9 sample is this feature rather smooth and shifted to 187 nm, while in the BE5H7 sample it falls at 165 nm. On the other hand, the spectral index of the far-UV extinction rise is rather stable for all the samples that we have examined ($\alpha \simeq 2.4$), except for the BE ($\alpha \simeq 2.1$) and AC5A6 ($\alpha \simeq 3.0$) samples.

Furthermore, we have to note that AC10H4 sample also presents a secondary peak at $\simeq 160$ nm. This result is not in agreement with the others. We tend to attribute this feature to an occasional instrument malfunctioning and/or to some local inhomogeneity of the specific LiF substrate.

4. DISCUSSION

Collisional growth is an efficient process in vapor condensation processes (Granquist & Buhrman 1976). Actually, temperature and pressure conditions are critical parameters in nucleation mechanisms (Katz 1970; Kamijo et al. 1975) and can influence the final grain dimensions: higher temperature and/or higher pressure favor coagulation and growth of particles. Furthermore, in consequence of collisional growth, the longer the collecting distance from the arc, the larger the grain mean size should be. Finally, the amount of dust collected on the samples might be relevant, as clumping of dust affects the extinction characteristics of grains (Huffman 1988; Wright 1989).

All the previous boundary experimental conditions may potentially influence the final extinction properties of amorphous carbon grains as these are critically dependent upon the morphology of the grains, as discussed below. In addition, the use of two different methods of production may evidence some relations between the nature of the grains and their final optical properties. We recall that in our experiments BE samples are produced in air starting from benzene, while AC grains are obtained by striking an arc between amorphous carbon electrodes in an inert Ar atmosphere.

The present results update the findings of a study performed by Colangeli et al. (1986) on a more limited number of AC samples. We note that the trend of the extinction curves of AC samples is generally in agreement with previous data. However, the main "hump" is now observed with no extra features, contrasted with how it was observed in the previous analysis. We tend to attribute the detection of those features to a poor correction for the LiF substrate transmittance. In fact, in the past the data were normalized to the transmittance of a

reference LiF window; its optical properties could have been different from those of the LiF substrate used to collect dust.

In the following we will propose some possible interpretations of the main features of amorphous carbon extinction curves: the UV hump at 240–260 nm, the minimum of extinction at 170–180 nm, and the far-UV rise.

4.1. *The UV Bump*

Graphite spherical grains have for a long time been considered responsible of the 220 nm interstellar extinction "hump" (see, e.g., Stecher & Donn 1965; Wickramasinghe & Guilliame 1965). In fact, Mie computations performed by using the optical constants of pure graphite provide a bump at the right position, attributed to a surface plasmon mode (Gilra 1971, 1972; Huffman 1977; Mathis et al. 1977). However, the presence of pure graphite grains in the interstellar medium has been criticized, while carbonaceous grains with a "disordered" structure still containing randomly oriented small graphitic islands appear more adequate to account for the "bump" (see, e.g., Czyzak et al. 1982; Hecht 1986; Bussoletti et al. 1987a).

We tend to attribute the hump observed in our amorphous carbon samples, falling at $\lambda_P = 240$–260 nm, to a surface plasmon resonance similar to that expected for graphite grains. This identification is further supported by the absence of any absorption feature at wavelengths longer than the peak position, as it appears from our results. This interpretation appears consistent with previous findings (Huffman 1977; Stephens 1980; Hecht 1986).

The results reported in § 3 provide evidence that the bump position for all AC samples is rather stable ($\lambda_P = 245 \pm 3$ nm), and it appears to be independent from the collecting distance, the operating pressure, and the collected mass amount, within our experimental limits. On the contrary, the samples produced by benzene burning (BE) show a broader peak shifted at around 260 nm.

At least two effects can be considered to interpret the previous results linked both to the morphological and to the chemical properties of the grains. According to theoretical studies (Perenboom, Wyder, & Meier 1981) and previous laboratory results (Genzel, Martin, & Kreibig 1975; Stephens 1980; Borghesi, Bussoletti, & Colangeli 1985) the peak position and band profile of surface resonances strongly depend upon dimensional parameters such as grain radii and size distribution. In particular, (1) the larger the grain radius, the longer the peak wavelength, and (2) the wider the size distribution, the smaller the height-to-width band ratio (Wickramasinghe, Lukes, & Dempsey 1974; Wickramasinghe & Nandy 1974). Actually, as already mentioned in § 2, AC grains are generally smaller ($\langle a \rangle = 40$ Å) than BE particles ($\langle a \rangle = 150$ Å). Therefore, the observed shift of λ_P from 245 to 260 nm might be interpreted as due to a size effect. On the other hand, the small variation of λ_P for the AC samples seems to suggest that these grains have similar average sizes, independent from pressure and collecting distance. The broad bump profile of AC3H9 and BE5H7 and the sharp peak of AC10H4 samples could be due to a wider and a narrower size distribution of the particles, respectively.

Very recently Wright (1989) has developed a theoretical model in which interstellar carbonaceous particles are simulated by "graphitic onions." These grains are formed by planes of graphite crystals perpendicular to a fixed axis of symmetry, and the rings surrounding this axis form the edges of the planes. It is interesting to note that computations of the optical properties of random fractal aggregates formed by "graphitic onions" under the discrete dipole approximation show an UV absorption feature. In particular, the peak shifts from 204 nm, for a single grain, to 240 nm, for aggregates, respectively.

Actually, TEM (transmission electron microscopy) images of amorphous carbon samples similar to those analyzed in UV spectroscopy have evidenced typical chainlike and fractal aggregations of grains (Borghesi et al. 1983). Therefore, according to the model proposed by Wright (1989), the bump in our spectra could be shifted at wavelengths longer than 220 nm as a consequence of "clustering" processes. As far as chemical properties of carbon grains are concerned, Hecht (1986) has proposed a physical model which suggests a relation of both the peak position and the shape of the UV hump with (1) the disorder degree and (2) the hydrogen content of the amorphous carbon samples (see also Bussoletti et al. 1987b). In particular, the peak position can shift toward shorter wavelengths according to the increasing graphitization of small amorphous carbon grains. Moreover, amorphous carbon grains rich in hydrogen content should not show any UV bump, as complete localization of π electrons inhibits the π plasmon resonance responsible for the UV bump at around 220–240 nm. As soon as the hydrogen is released, the resonance becomes active (McKenzie et al. 1983; Fink et al. 1984).

On the basis of this model, the shallow bump in BE spectra could be interpreted with a high hydrogenation of the samples; on the contrary, AC grains should contain a minor amount of hydrogen. Furthermore, the 245 nm peak position appears consistent with the properties of nongraphitic, low-density forms of carbon (Ledger & Suddeth 1960; Williams & Arakawa 1972; Hecht 1986).

4.2. *The Far-UV Profile*

According to Fink et al. (1984) a $\sigma + \pi$ plasmon produces a strong absorption peak around 540–520 Å in the spectrum of hydrocarbon-plasma–generated carbon films. A similar feature, shifted at around 800 Å, is present in the absorption efficiency spectrum of the "astronomical graphite" theoretically synthetized by Draine & Lee (1984). More generally, such a short-wavelength feature can be expected for any kind of carbonaceous grains, and, unlike for the π plasmon responsible of the 220–260 nm hump, the hydrogenation of the particles does not inhibit the presence of the $\sigma + \pi$ band (Fink et al. 1984; Hecht 1986). However, hydrogenated amorphous carbon grains would be expected to have the band shifted slightly to the red (Hecht 1986).

Following the previous considerations we might interpret the far-UV extinction rise observed for our amorphous carbon samples as the long-wavelength wing of the previously mentioned high-energy plasmon resonance. In this scenario, the minimum of extinction at λ_M would represent the turnover point between the two main spectral features. Therefore, it seems reasonable that its wavelength position can be rather variable. In fact, λ_M can be affected both by the short-wavelength profile of the bump and by the actual position of the high-energy resonance. Both these elements may change according to the detailed chemical and/or morphological properties of the dust samples.

On the other hand, we have to recall that we deal with samples formed by solid grains, and, therefore, scattering effects may be relevant for particles which are small compared to the wavelength of the incident radiation. Actually, the AC and BE grain mean sizes fulfill this constraint. Therefore, in

principle, we cannot exclude the possibility that scattering might contribute to produce the far-UV trend observed for our samples. Nevertheless, we have to recall that the particles occur as fluffy clusters, whose dimensions are comparable with wavelength. Therefore, specific scattering measurements are needed in order to assess definitely the possible incidence of this process on the total extinction.

5. ASTROPHYSICAL IMPLICATIONS AND CONCLUSIONS

Taking into account the discussion in § 4, it appears possible to consider amorphous carbon grains similar to those analyzed in our experiments among the candidates which can simulate interstellar and/or circumstellar carbonaceous grains. In fact, as reported in § 1, circumstellar extinction around carbon-rich stars such as Abell 30 (Greenstein 1981), RCrB and RY Sgr (Hecht et al. 1984), and HD 213985 (Buss et al. 1989) does show an absorption "bump" at 230–250 nm, an extinction minimum at around 180 nm, and a linear rise in the far-UV.

On the other hand, according to Jura (1986), carbon-rich stars eject a large amount of circumstellar dust into the interstellar medium. Therefore, it appears likely that interstellar carbon-based grains are some sort of modified form of the circumstellar dust (Hecht 1986). Under this hypothesis, several mechanisms could produce the shift of the peak wavelength of the "bump" from 240 to 220 nm.

The clustering effect discussed by Wright (1989) could be active in circumstellar environment but not with the same relevance in the interstellar medium, so that the shift could be produced by variations in the degree of aggregation of the grains. The presence of hydrogen might be required in order to produce the 220 nm feature. In fact, hydrogen atoms bound to carbon atoms in the grains could prevent the aggregation of "onions" to form large clusters so that particles containing ordered substructures would be able to produce the 220 nm feature.

Alternatively, hydrogen could change the overall dielectric constants of the material as suggested by various authors (Hecht et al. 1984; Hecht 1986; Goebel 1987; Sorrell 1990). As already discussed in § 4, amorphous carbon grains should or should not produce the 220–240 nm bumps according to their degree of hydrogenation. Moreover, the residual crystallinity of amorphous carbon grains, produced around carbon stars, could be modified in the interstellar medium by irradiation and/or shock processes. The effect would be a shift of the peak to shorter wavelength (see, e.g., Hecht 1986; Sorrell 1990).

Finally, it is worthwhile to note that amorphous carbon grains appear able to simulate both the bump and the far-UV rise of the interstellar extinction curve. As in our scenario these two features are attributed to different characteristics of the same carbonaceous grains, they are not necessarily correlated. This result is in agreement with astronomical observations: depending on the local conditions, the physical, chemical, and/or structural properties of the basic carbonaceous grains may vary. Therefore, the overall profile of the extinction curves will be different. This picture does not appear to contrast with that proposed by Hecht (1986), who invokes two separate populations of carbonaceous grains to simulate the bump and the far-UV curvature. In fact, those two classes could be considered as two different modifications of the same starting material.

We express our thanks to N. Zema, responsible for the UV line at the PULS National Facility, for the availability of the laboratory structures, his helpful assistance during the measurements, and stimulating discussions. This work has been supported under contracts by ASI, CNR, GIFCO, and the Ministero Pubblica Istruzione.

REFERENCES

Borghesi, A., Bussoletti, E., & Colangeli, L. 1985, A&A, 142, 225
Borghesi, A., Bussoletti, E., Colangeli, L., Minafra, A., & Rubini, F. 1983, Infrared Phys., 23, 85
Buss, R. H., Lamers, H., & Snow, T. P. 1989, ApJ, 347, 977
Bussoletti, E., Colangeli, L., Borghesi, A., & Orofino, V. 1987a, A&AS, 70, 257
Bussoletti, E., Colangeli, L., & Orofino, V. 1987b, ApJ, 321, L87
Colangeli, L., Capozzi, V., Bussoletti, E., & Minafra, A. 1986, A&A, 168, 349
Czyzak, S. J., Hirth, J. P., & Tabak, R. G. 1982, Vistas Astron., 25, 337
Czyzak, S. J., & Santiago, J. J. 1973, Ap&SS, 23, 443
Draine, B. D. 1989, in Interstellar Dust, ed. L. J. Allamandola & A. G. G. M. Tielens (Dordrecht: Kluwer), 313
Draine, B., & Lee, H. M. 1984, ApJ, 285, 89
Duley, W. W., Jones, A. P., & Williams, D. A. 1989, MNRAS, 236, 709
Fink, J., Müller-Heinzerling, T., Pfüger, J., Scheerer, B., Dischler, B., Koidl, P., Bubenzer, A., & Sah, R. 1984, Phys. Rev. B, 30, 4713
Genzel, L., Martin, T. P., & Kreibig, U. 1975, Z. Phys., B21, 339
Gilra, D. P. 1971, Nature, 299, 237
———. 1972, in The Scientific Results from the Orbiting Astronomical Observatory *OAO-2*, NASA SP-310, 295
Goebel, J. H. 1987, in Polycyclic Aromatic Hydrocarbons and Astrophysics, ed. A. Leger, L. d'Hendecourt, & N. Boccara (Dordrecht: Reidel), 329
Granquist, C. G., & Buhrman, R. A. 1976, J. Appl. Phys., 47, 2200
Greenberg, J. M. 1986, in Light on Dark Matter, ed. F. P. Israel (Dordrecht: Reidel), 177
Greenstein, J. L. 1981, ApJ, 245, 124
Hecht, J. 1986, ApJ, 305, 817
Hecht, J., Holm, A. V., Donn, B., & Wu, C.-C. 1984, ApJ, 280, 228
Hong, S. S., & Greenberg, J. M. 1980, A&A, 88, 194
Huffman, D. R. 1977, Adv. Phys., 26, 129
———. 1988, in Experiments on Cosmic Dust Analogues, ed. E. Bussoletti, C. Fusco, & G. Longo (Dordrecht: Kluwer), 25
Jura, M. 1986, ApJ, 303, 327
Kamijo, F., Nakada, Y., Iguchi, T., Fujimoto, M. K., & Takada, M. 1975, Icarus, 26, 102
Katz, J. L. 1970, J. Stat. Phys., 2, 137
Koike, C., Hasegawa, H., & Manabe, A. 1980, Ap&SS, 67, 495
Ledger, L. B., & Suddeth, J. A. 1960, J. Appl. Phys., 31, 1422
Lewis, R. S., Anders, E., & Draine, B. T. 1989, Nature, 339, 117
Massa, D., & Savage, B. 1989, in Interstellar Dust, ed. L. J. Allamandola & A. G. G. M. Tielens (Dordrecht: Kluwer), 3
Mathis, J. S., Rumpl, W., & Nordsieck, K. H. 1977, ApJ, 217, 425
McKenzie, D. R., McPhedran, R. C., Savvides, N., Cockayne, D. J. H. 1983, Thin Solid Films, 108, 247
Perenboom, J. A. A. J., Wyder, P., & Meier, F. 1981, Phys. Rep., 78, 173
Seki, J., & Hasegawa, H. 1981, Prog. Theor. Phys., 66, 903
Snow, T. P., Buss, R. H., Gilra, D. P., & Swings, J. P. 1987, ApJ, 321, 921
Sorrell, W. H. 1990, MNRAS, 243, 570
Stecher, T. P., & Donn, B. 1965, ApJ, 142, 1683
Stephens, J. R. 1980, ApJ, 237, 450
Wickramasinghe, N. C., & Guilliame, P. 1965, Nature, 207, 366
Wickramasinghe, N. C., Lukes, T., & Dempsey, M. J. 1974, Ap&SS, 30, 315
Wickramasinghe, N. C., & Nandy, K. 1974, Ap&SS, 26, 123
Williams, M. W., & Arakawa, E. T. 1972, J. Appl. Phys., 43, 3460
Wright, E. L. 1989, ApJ, 346, L89
Yamamoto, T., & Hasegawa, H. 1977, Prog. Theor. Phys., 58, 816